Thermodynamic analysis and optimization of quality-improving heat pumps coupled with organic Rankine cycle for mid-low temperature geothermal power generation[#]

Yongqiang Li, Yongliang Zhao*, Ming Liu and Junjie Yan

1 State Key Laboratory of Multiphase Flow in Power Engineering, Xi'an Jiaotong University, Xi'an 710049, China

yl.zhao@mail.xjtu.edu.cn

ABSTRACT

In order to achieve efficient utilization of mid-low temperature geothermal resources, three different types of quality-improving heat pumps coupled with organic Rankine cycle for mid-low temperature geothermal power generation system are designed and discussed. Initially, mathematical models of each system as well as a thermodynamic evaluation system are developed. Secondly, by optimizing the operating parameters with the optimization goal of maximum overall exergy efficiency, the optimal operation states for each system are obtained. Finally, thermodynamic performance parameters of each system are compared and appropriate application scenarios for both systems are discussed. The results reveal that the optimal operating conditions for AHT-ORC-A, AHT-ORC-B, and CHP-ORC are achieved when the heat pumps elevate the temperatures to 117.0 °C, 104.8 °C, and 115.0 °C respectively. Meanwhile, their overall exergy efficiencies are 38.93%, 53.07%, and 35.40% respectively. AHT-ORC-A boasts the highest output power density, while CHP-ORC has the lowest power density. Therefore, from the perspective thermodynamic performance, AHT-ORC outperforms CHP-ORC. Furthermore, when the condensation heat from AHT is utilized to meet the heating demands of users, a more efficient utilization of energy can be achieved.

Keywords: Mid-low temperature geothermal, System optimization, Thermodynamic design, Heat pump, Organic Rankine Cycle

NONMENCLATURE

Abbreviations	
ADAPEN	Advances in Applied Energy
AHT	Absorption Heat Transformer
CHP	Compression Heat Pump

COP	Coefficient of Performance
ORC	Organic Rankine Cycle
GWP	Global Warming Potential
ODP	Ozone Depletion Potential
Symbols	
E	Exergy, [J]
EFF	Efficiency of ORC
Ex	Overall Exergy Efficiency
h	Enthalpy, [J·kg^{-1}]
m	Mass Flow, [kg·s^{-1}]
Q	Heat, [W]
T	Temperature, [K]
W	Power, [W]
η	Isentropic Efficiency

1. INTRODUCTION

The development and utilization of geothermal energy are characterized by continuous and stable energy supply, and renewability [1], additionally, it boasts unique advantages such as low cost, immunity to climate change, and uninterrupted operation, without the need for energy storage systems, thereby complementing the fluctuating wind and solar energy [2]. Consequently, vigorously promoting geothermal power generation in accordance with local conditions holds great significance for improving the structure of renewable energy and ensuring a reliable and stable energy supply [3].

Although research in traditional high-temperature geothermal power generation has made significant progress and achieved commercial applications, the development of mid-low temperature geothermal power generation, which boasts a wider distribution and richer reserves, lags behind. The advancements in this field have been relatively slow. Notably, in various regions worldwide, there exist mid-low temperature geothermal sources along coastal areas and shallow sea depths that

---

can be economically harnessed in multifaceted energy generation systems [4]. Furthermore, unlike conventional high-temperature geothermal sources, the water derived from these mid-low temperature sources is non-toxic due to their shallow depths [5]. Hence, there is a pressing need to actively explore and develop mid-low temperature geothermal generation technologies [6].

Current mid-low temperature power generation technologies encompass: flash cycle [7], thermoelectric power generation [8], Kalina cycle [9] and organic Rankine cycle (ORC) [10]. However, these technologies face several technical bottlenecks in the field of mid-low temperature geothermal power generation: Firstly, the power generation efficiency is not sufficiently high [11]; secondly, reliability and service life need improved [12], with issues such as working fluid decomposition, leakage, component corrosion, and aging failure arising after prolonged operation [13]; lastly, due to the suboptimal efficiency and reliability, the economics are poor, making it difficult to attract investment, thereby constraining the development of mid-low temperature geothermal power generation [14].

In order to achieve efficient utilization of mid-low temperature geothermal resources, three different types of mid-low temperature geothermal power generation system are designed in this study. Firstly, mathematical models as well as a thermodynamic evaluation system are developed. Secondly, by optimizing the operating parameters with the optimization goal of maximum overall exergy efficiency, the optimal operation states are obtained. Finally, thermodynamic performance parameters of each system are compared.

2. SYSTEM DESIGN

2.1 System configurations

To improve the performance, ORC is coupled with quality-improving heat pumps. The first configuration is to couple a absorption heat transformer (AHT) with ORC, as shown in Fig. 1(a). Depending on whether the condenser of the heat pump supplies heat, this configuration can be divided into two operating modes: (1) absorption heat transformer-organic Rankine cycle without heat supply (AHT-ORC-A); and (2) absorption heat transformer-organic Rankine Cycle with heat supply (AHT-ORC-B). Another configuration is compression heat pump-organic Rankine cycle (CHP-ORC), as shown in Fig. 1(b). In order to achieve better performance, both heat pumps and ORCs in these configurations are equipped with regenerators.
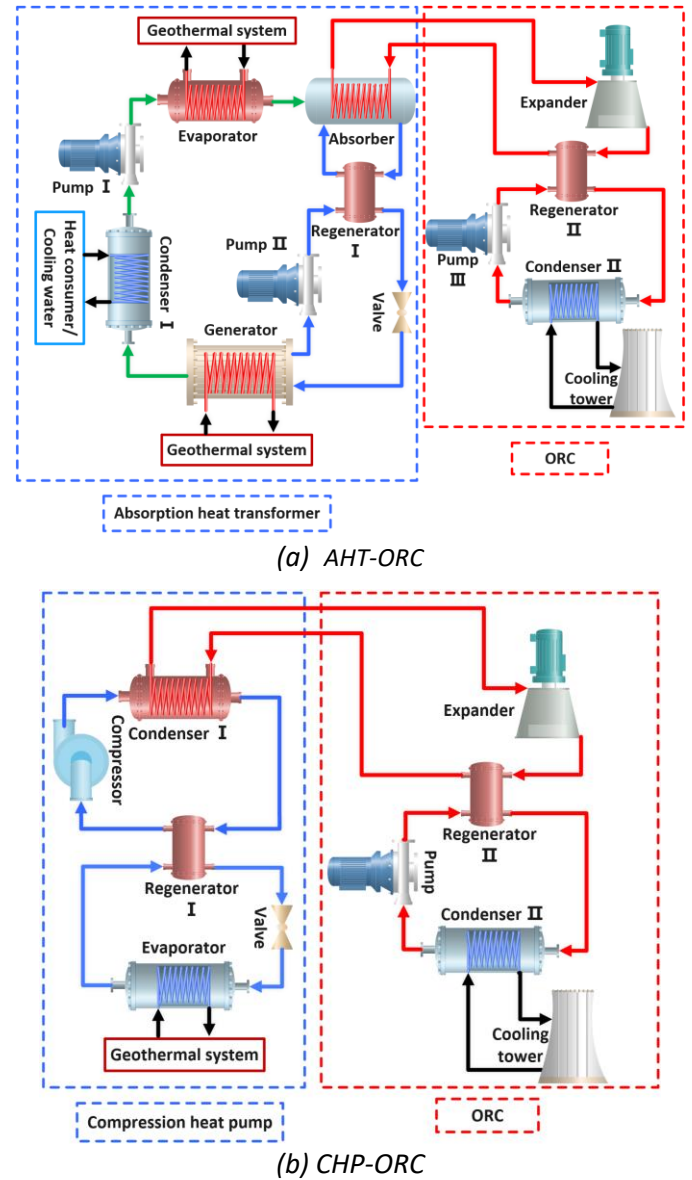

(a) AHT-ORC

(b) CHP-ORC

Fig. 1 Layout of two power generation systems

2.2 Section of working fluids

LiBr/H_2O, as the most commonly used working fluid for AHP, boasts remarkable advantages such as environmental friendliness, high efficiency, stability, durability, and economic long-term operation [15]. Therefore, LiBr/H_2O is selected as the working fluid for the AHT, with its concentration determined through optimization calculations. R245fa and R1233zd(e) achieve high efficiency in ORC [16], and due to their low global warming potential (GWP) and zero ozone depletion potential (ODP), they meet environmental requirements and have been widely used in mid-low temperature power generation [17]. Furthermore, the saturation curves of these two working fluids are close. Thus, R1233zd(e) and R245fa are selected as the working fluid for CHP and ORC, respectively.

3. THERMODYNAMIC MODELLING

In this section, the thermodynamic models of the AHT-ORC and CHP-ORC are presented. The following assumptions are considered to facilitate the modelling:

(1) Changes in kinetic and potential energy of the working fluids are disregarded.

(2) Pressure drops and heat dissipation in each pipe and equipment are omitted.

(3) The lithium bromide solutions in AHT at the outlets of the generator and absorber are saturated.

(4) The pump work in AHT is neglected.

(5) Working states of the expander are specified as isentropic expansion process and working states of the pump and compressor are specified as isentropic compression process.

3.1 Mathematical modeling

The AHT-ORC and CHP-ORC mainly comprise fluid machineries (pump, compressor, expander), valve, heat exchanger (condenser, evaporator, regenerator), and generator/absorber. The mathematical models of the above components are summarized in Table 1.

Table 1 Mathematical models of components.

Component	Formula
Fluid machinery	$\dot{W} = \dot{m}(h_{out} - h_{in})$ $h_{out} = h_{in} + (h_{out,is} + h_{in})/\eta$
Valve	$h_{out} = h_{in}$
Heat exchanger	$\dot{Q} = \dot{m}_h(h_{in} - h_{out}) = \dot{m}_c(h_{out} - h_{in})$
Generator/ Absorber	$\dot{Q} = \sum \dot{m}_{out}h_{out} - \sum \dot{m}_{in}h_{in}$ $\sum \dot{m}_{out} = \sum \dot{m}_{in}$

where η means the isentropic efficiencies of the compressor, expander and pump; h means the specific enthalpy of the fluid, kJ·kg^{-1}; $\dot{m}$ is the mass flow, kg·s^{-1}; and $\dot{W}$ means the power of turbomachinery, kW; $\dot{Q}$ means heat transfer power, kW. The subscript in and out mean the inlet and outlet of the components, h and c mean the hot and cold side, respectively.

3.2 Performance indicators

Because there are both geothermal input and electric work input in the heat pumps, and the grade of geothermal energy is lower than that of electricity, the coefficient of performance (COP) of the heat pumps is defined as follows:

$$COP = \frac{Q_{out}}{Q_{in}} = \frac{Q_{Hp}}{Q_{Geo} + \frac{Q_{Geo}}{E_{Geo}} \times \dot{W}_{Cmp}} \qquad (1)$$

where Q_{Hp} represents the high-quality heat produced by the heat pump, W; Q_{Geo} represents the heat input into the system from geothermal water, W; E_{Geo} is the exergy from geothermal water consumed by the heat pumps, W; and $\dot{W}_{Cmp}$ is the consumed power in compressors, W.

For the ORC, the cycle efficiency is defined as the ratio of the net work output to the input heat:

$$EFF = \frac{P_{out}^{ORC}}{Q_{in}^{ORC}} = \frac{\dot{W}_{Exp} - \dot{W}_{Cmp} - \dot{W}_{Pmp}}{Q_{Hp}} \qquad (2)$$

where P_{out}^{ORC} represents the net output power of ORC, W; Q_{in}^{ORC} is the heat input to ORC, J; $\dot{W}_{Exp}$, $\dot{W}_{Cmp}$ and $\dot{W}_{Pmp}$ are the output power of expanders, the input power of compressors and pumps, respectively, W.

The overall exergy efficiency of the system is the ratio of output exergy to input exergy:

$$Ex = \frac{E_{out}}{E_{in}} = \frac{P_{out}^{ORC} + E_{Heat}}{E_{Geo}} \qquad (3)$$

where E_{Heat} represents the exergy provided by the heat pumps for heat consumer, W.

3.3 Optimization method

In this study, the thermal properties of R245fa are obtained from the REFPROP database, and the physical properties of the lithium bromide solutions are calculated using the fitting formula in the literature [18].

The models are created using MATLAB and optimized with the objectives of the highest overall exergy efficiency. The algorithm is used as following:

$$\min_{x} f(x) \text{ such that} \begin{cases} c(x) \leqslant 0 \ (\text{nonlinear inequality constraints}) \\ ceq(x) = 0 \ (\text{nonlinear equality constraints}) \\ A \cdot x \leqslant b \ (\text{linear inequality constraints}) \\ Aeq \cdot x = beq \ (\text{linear equality constraints}) \\ lb \leqslant x \leqslant ub \ (\text{range of optimized parameters}) \end{cases}$$

where the nonlinear inequality constraints mainly include the working temperature limit of the minimum heat exchange temperature difference to prevent pinch points, and limit of concentration of lithium bromide solutions. The range of optimized parameters include upper and lower limits for the parameter groups to be optimized, namely state of the working fluids in the components.

4. RESULTS AND DISCUSSION

In this study, the outlet and inlet temperatures of the geothermal water are 90 °C and 80 °C, respectively, and the outlet and inlet temperatures of the hot water in the AHT-ORC-B are 35 °C and 50 °C, respectively. The rest of the boundary conditions are shown in Table 2.

Table 2 Main parameters and setting values.

Main parameters	Values
Ambient temperature	25.0 °C
Ambient pressure	0.105 MPa
Compressor isentropic efficiency	0.90
Pump isentropic efficiency	0.90
Expander isentropic efficiency	0.85
Pinch point temperature difference	5.0 °C
Mass flow of working fluids in heat pumps	1.0 kg/s

After inputting the parameters into the program and running the optimization program, the parameters of each configuration are optimized by the Fmincon algorithm to obtain the highest overall exergy efficiency.

The *T-p* diagrams of AHT and *T-s* diagrams of ORC in AHT-ORC are shown in Fig. 2. The black dotted line is the saturation curve of water, and the black dashed line is the saturation curve of R245fa. The blue lines represent the lithium bromide solutions in the generator and absorber. The blue dashed lines indicate the regeneration and pressure change processes of lithium bromide solutions in the AHT. The green line represents the water in the AHT. The purple dashed lines indicate that the water leave or enter the lithium bromide solutions. Red lines represent ORC process, and red dotted lines indicate the regeneration process in ORC.

As shown in Fig. 2, the AHT in AHT-ORC-A elevates the temperature to 117.0 °C, while the AHT in AHT-ORC-B achieves a lower temperature of 104.8 °C. This temperature discrepancy arises from the fact that when the heat released from the AHT condenser is utilized for heating purposes, the temperature of outlet superheated steam and in let saturated water need to be higher, resulting in an increase of condensing pressure. And an elevated condensing pressure leads to a decrease in the concentration of the solution at the outlet of the generator, thereby weakening the generation capacity of the generator. This directly impacts the temperature enhancement performance of AHT. What's more, the absence of superheating in ORC can be attributed that the temperature of heat source generated by AHT is stable. If superheating occurs in ORC, it would result in a greater loss of energy quality when the ORC working fluid absorbs the high-grade heat source produced by AHT.
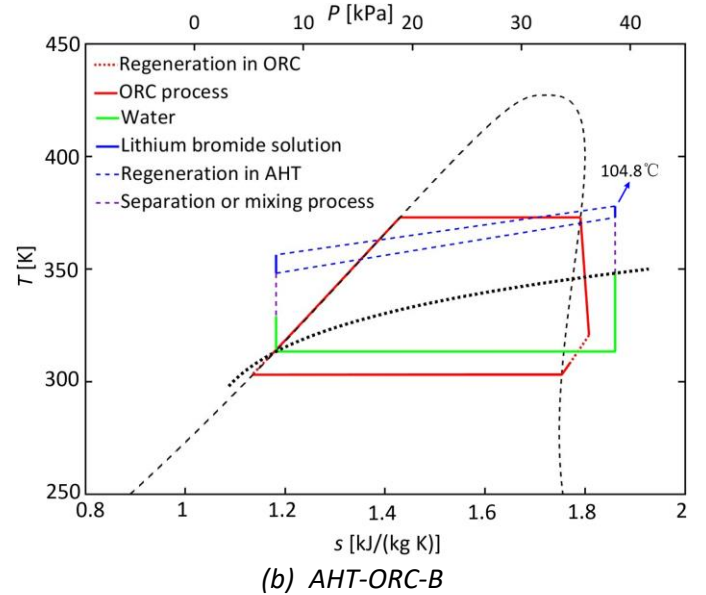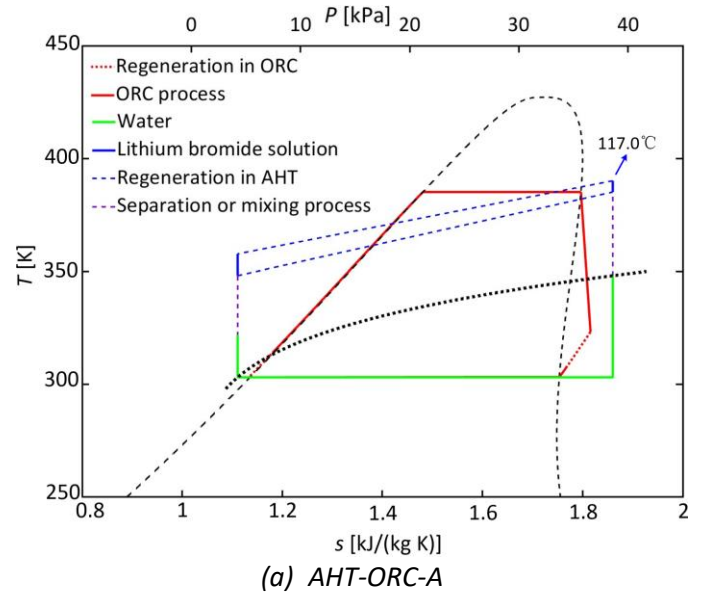

(a) AHT-ORC-A

(b) AHT-ORC-B

Fig. 2 T-p diagrams of AHT and T-s diagrams of ORC

The *T-s* diagrams CHP-ORC is shown in Fig. 3. The left black dashed line is the saturation curve of R1233zd(e), and the right black dashed line is the saturation curve of R245fa. The blue lines red lines represent the CHP and ORC process. Blue and red dotted lines indicate the regeneration process in CHP and ORC, respectively.

As shown in Fig. 3, the CHP releases heat to the ORC after raising the temperature to 115.0 °C. The saturation curves of R1233zd(e) and R245fa are close, with R1233zd(e) slightly shifted to the left, resulting in great temperature matching in the high-temperature heat exchange section. However, in the low-temperature heat exchange section, due to the low inlet temperature of the ORC evaporator, the higher-temperature heat from CHP is used to supply the low-temperature section of the ORC, leading to a considerable loss of energy quality.
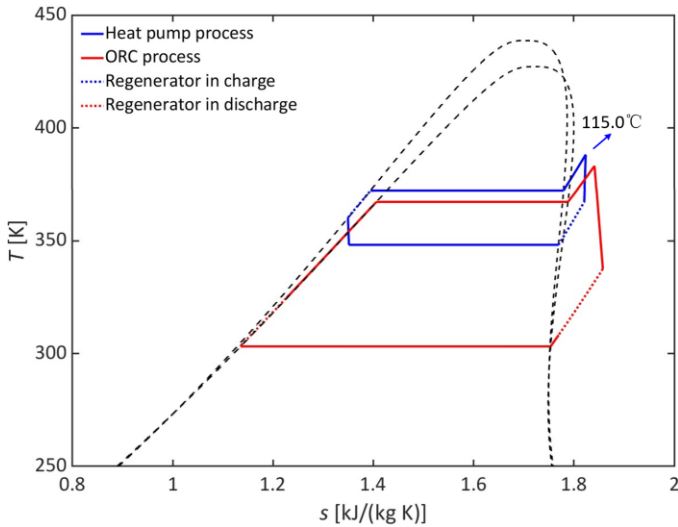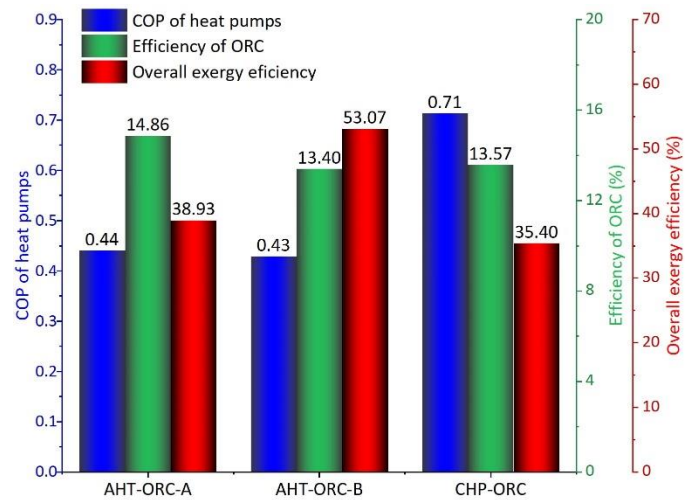
Fig. 3 T-s diagram of CHP-ORC

(a) Thermodynamic performance

(b) Net output power and mass flow

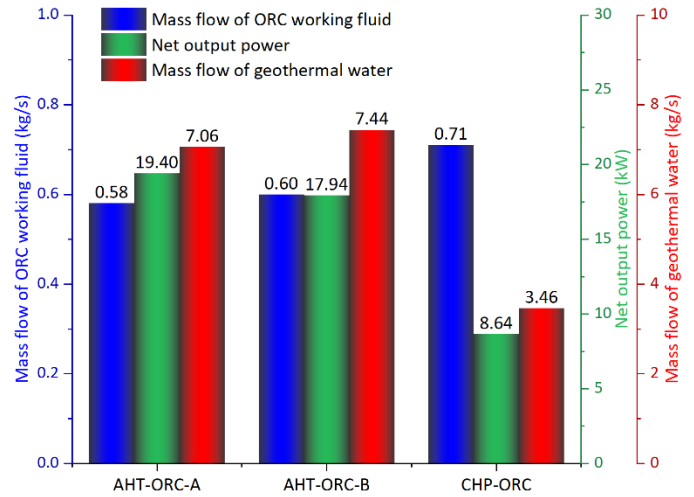*Fig. 4 Comparison of three configurations*

A series of comparisons for each configuration are presented in Fig. 4. From Fig. 4(a), the CHP-ORC exhibits the highest COP. Despite the lower temperature lift achieved by the AHT in AHT-ORC-B compared to AHT-ORC-A, the COP of AHT-ORC-B is slightly lower than that of AHT-ORC-A. This discrepancy arises from the necessity to elevate the condensation temperature in AHT-ORC-B to meet heating demands, which increases the condensation pressure, weakening its heating capacity and reducing the production of high-grade heat.

The efficiency of the ORC decreases sequentially from AHT-ORC-A, AHT-ORC-B to CHP-ORC, primarily due to the successive decline in the temperature of the high-grade heat source generated by the heat pumps. Among the three systems, CHP-ORC demonstrates the lowest overall exergy efficiency, merely 35.40%, due to the considerable power consumption of the compressor in CHP. Conversely, AHT-ORC-B boasts the highest overall exergy efficiency, reaching 53.07%, as it utilizes low-grade heat for heat supply, thereby achieving optimal energy utilization.

From Fig. 4(b), with the same working fluid flow mass in the heat pumps set at 1.0 kg/s, AHT-ORC-A requires the least amount of ORC working fluid, which is 0.58 kg/s, and achieves the maximum net output power of 19.40 kW. Consequently, this configuration boasts the highest output power density. Upon introducing heat supply, both ORC working fluid required and the geothermal water consumption increase slightly, while the net output power has a slight decline. CHP-ORC need the highest quantity of ORC working fluid, reaching 0.71 kg/s, and consumes the least amount of geothermal water, only 8.64 kg/s. Simultaneously, it yields the lowest net output power of 3.46 kW, thereby resulting in the lowest power density among the configurations.

5. CONCLUSIONS

In this study, three different types of mid-low temperature geothermal power generation system are developed and modeled. By optimizing the operating parameters and comparing the different configurations, the following conclusions are obtained:

(1) The optimal operating conditions for AHT-ORC-A, AHT-ORC-B, and CHP-ORC are achieved when the heat pumps elevate the temperatures to 117.0 °C, 104.8 °C, and 115.0 °C, respectively.

(2) Their optimal overall exergy efficiencies are 38.93%, 53.07%, and 35.40%, respectively. Therefore, from the perspective of thermodynamic performance, AHT-ORC outperforms CHP-ORC. Furthermore, when the condensation heat from AHT is utilized to meet the heating demands of users, a more efficient utilization of energy can be achieved.

(3) AHT-ORC-A requires the least amount of ORC working fluid, which is 0.58 kg/s, and achieves the

maximum net output power of 19.40 kW. Consequently, this configuration boasts the highest output power density. Upon introducing heat supply, both ORC working fluid required and the geothermal water consumption increase slightly, while the net output power has a slight decline. CHP-ORC need the highest quantity of ORC working fluid, reaching 0.71 kg/s. Simultaneously, it yields the lowest net output power of 3.46 kW, thereby resulting in the lowest power density.

ACKNOWLEDGEMENT

REFERENCE

[1] Templeton JD, Ghoreishi-Madiseh SA, Hassani F, Al-Khawaja MJ. Abandoned petroleum wells as sustainable sources of geothermal energy. Energy. 2014;70:366-73.

[2] Shortall R, Davidsdottir B, Axelsson G. Geothermal energy for sustainable development: A review of sustainability impacts and assessment frameworks. Renewable & Sustainable Energy Reviews. 2015;44:391-406.

[3] Soltani M, Kashkooli FM, Souri M, Rafiei B, Jabarifar M, Gharali K, et al. Environmental, economic, and social impacts of geothermal energy systems. Renewable & Sustainable Energy Reviews. 2021;140.

[4] Behnam P, Arefi A, Shafii MB. Exergetic and thermoeconomic analysis of a trigeneration system producing electricity, hot water, and fresh water driven by low-temperature geothermal sources. Energy Conversion and Management. 2018;157:266-76.

[5] Bundschuh J, Ghaffour N, Mahmoudi H, Goosen M, Mushtaq S, Hoinkis J. Low-cost low-enthalpy geothermal heat for freshwater production: Innovative applications using thermal desalination processes. Renewable & Sustainable Energy Reviews. 2015;43:196-206.

[6] Hu B, Guo JJ. Experimental study on medium and low temperature geothermal ammonia power generation system based on vertical tube falling film. Energy Reports. 2022;8:723-9.

[7] Luo C, Zhao J, Gong YL, Wang YZ, Ma WB. ENERGY EFFICIENCY COMPARISON BETWEEN GEOTHERMAL POWER SYSTEMS. Thermal Science. 2017;21:2633-42.

[8] Alegría P, Catalán L, Araiz M, Erro I, Astrain D. Design and optimization of thermoelectric generators for harnessing geothermal anomalies: A computational model and validation with experimental field results. Applied Thermal Engineering. 2024;236.

[9] Li SL, Dai YP. Thermo-economic comparison of Kalina and CO_2 transcritical power cycle for low temperature geothermal sources in China. Applied Thermal Engineering. 2014;70:139-52.

[10] Wang SK, Liu C, Zhang SJ, Li QB, Huo ER. Multi-objective optimization and fluid selection of organic Rankine cycle (ORC) system based on economic-environmental-sustainable analysis. Energy Conversion and Management. 2022;254.

[11] Fiaschi D, Manfrida G, Rogai E, Talluri L. Exergoeconomic analysis and comparison between ORC and Kalina cycles to exploit low and medium-high temperature heat from two different geothermal sites. Energy Conversion and Management. 2017;154:503-16.

[12] Oh J, Park Y, Lee H. Development of a fully deterministic simulation model for organic Rankine cycle operating under off-design conditions. Applied Energy. 2022;307.

[13] Ding Y, Liu C, Zhang C, Xu XX, Li QB, Mao LF. Exergoenvironmental model of Organic Rankine Cycle system including the manufacture and leakage of working fluid. Energy. 2018;145:52-64.

[14] Xie HP, Li CB, Zhou T, Chen JL, Liao JX, Ma JC, et al. Conceptualization and evaluation of the exploration and utilization of low/medium-temperature geothermal energy: a case study of the Guangdong-Hong Kong-Macao Greater Bay Area. Geomechanics and Geophysics for Geo-Energy and Geo-Resources. 2020;6.

[15] Sun J, Fu L, Zhang SG. A review of working fluids of absorption cycles. Renewable & Sustainable Energy Reviews. 2012;16:1899-906.

[16] Liu Q, Duan YY, Yang Z. Performance analyses of geothermal organic Rankine cycles with selected hydrocarbon working fluids. Energy. 2013;63:123-32.

[17] Abadi GB, Yun E, Kim KC. Experimental study of a 1 kw organic Rankine cycle with a zeotropic mixture of R245fa/R134a. Energy. 2015;93:2363-73.

[18] Mingsheng J. Several Main Calculating Equations of Properties Parameter of LiBr-H_2O. Journal of Zhanjiang Ocean University. 2002.